

Electroweak corrections to squark–anti-squark pair production at the LHC

W. Hollik and E. Mirabella

Max-Planck-Institut für Physik (Werner Heisenberg Institut) Föhringer Ring 6, D-80805 München, Germany

Abstract. Presented are the complete NLO electroweak contributions to the production of diagonal squark–anti-squark pairs at the LHC. We discuss their effects for the production of squarks of the first two generations, in different SUSY scenarios.

Keywords: MSSM, NLO Computations, Hadronic Colliders

INTRODUCTION

If Supersymmetry (SUSY) is realized at the TeV-scale or below it will be probed at the Large Hadron Collider (LHC). Experimental studies will be possible through the direct production of SUSY particles. In particular colored particles will be copiously produced, so squark and gluino production can play an important role in the hunting for SUSY. In the following we will focus on the production of a squark–anti-squark pair,

$$PP \rightarrow \tilde{Q}^a \tilde{Q}^{a*} X \quad (\tilde{Q} \neq \tilde{t}, \tilde{b}). \quad (1)$$

The lowest order cross section for the process (1) is of $\mathcal{O}(\alpha_s^2)$ and was computed in the early 1980's [1–4]. The dominant NLO corrections, of $\mathcal{O}(\alpha_s^3)$, were calculated in Ref. [5]. They are positive and sizable, typically from 20% to 30% of the lowest order prediction.

There are also $\mathcal{O}(\alpha_s \alpha)$ and $\mathcal{O}(\alpha^2)$ corrections to diagonal squark pair production from $q\bar{q}$ annihilation [6]. Contributions of $\mathcal{O}(\alpha^2)$ are obtained squaring the tree-level EW graphs while $\mathcal{O}(\alpha_s \alpha)$ corrections arise from the interference of tree-level EW diagrams with the tree-level QCD ones. The latter vanish for $\tilde{Q} = \tilde{t}$, but they can become sizable if $\tilde{Q} \neq \tilde{t}$.

NLO electroweak (EW) contributions were found to be significant in the case of top-squark pair production, with effects up to 20% [7, 8]. In the case of the process (1) NLO EW corrections can reach the same size as the tree-level EW contributions of $\mathcal{O}(\alpha_s \alpha)$ and $\mathcal{O}(\alpha^2)$ [9].

EW CONTRIBUTIONS

Diagrams and corresponding amplitudes for the EW contributions to the process (1) are generated using `FeynArts` [10, 11] while the algebraic manipulations and the numerical evaluation of the loop integrals are performed with the help of `FormCalc` and

`LoopTools` [12, 13]. IR and Collinear singularities are regularized within mass regularization.

Tree level EW contributions

Tree-level EW contributions to the process (1) are of $\mathcal{O}(\alpha_s \alpha)$ and $\mathcal{O}(\alpha^2)$. The interference of the tree-level electroweak and tree-level QCD diagrams give rise to terms of order $\mathcal{O}(\alpha_s \alpha)$, while $\mathcal{O}(\alpha^2)$ terms are obtained squaring the aforementioned tree-level EW graphs. We consider also the photon-induced partonic process $\gamma g \rightarrow \tilde{Q}^a \tilde{Q}^{a*}$, which contributes at $\mathcal{O}(\alpha_s \alpha)$, owing to the non-zero photon density in the proton which stems from the inclusion of NLO QED effects into the DGLAP equations for the parton distribution functions (PDFs).

NLO EW contributions

NLO EW corrections arise from three different channels, gluon fusion, quark–anti-quark annihilation, and quark–gluon fusion channels.

Virtual Corrections

Virtual corrections originate from the interference of the tree-level diagrams with the one-loop EW graphs. In the case of $q\bar{q}$ annihilation channels, the interference between tree-level EW diagrams and QCD one loop graphs has to be considered as well. Particularly interesting is the $q\bar{q}$ annihilation channel when the quark belongs to the same SU(2) doublet of the produced squark. In this case many types of interferences occur between amplitudes of $\mathcal{O}(\alpha_s \alpha)$ and $\mathcal{O}(\alpha_s)$ and between $\mathcal{O}(\alpha_s^2)$ and $\mathcal{O}(\alpha)$ amplitudes. This is related to the presence of EW tree-level diagrams with t -channel neutralino and chargino exchange and of QCD tree-level diagrams with

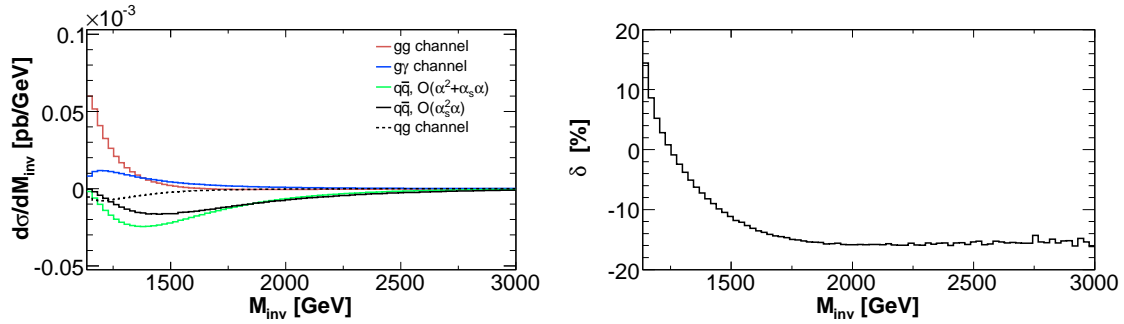


FIGURE 1. Invariant mass distribution of $u^L u^{L*}$ production for the SUSY parameter point corresponding to SPS1a'. The left panel shows the contributions of the different channels. δ is the EW contribution relative to the LO one.

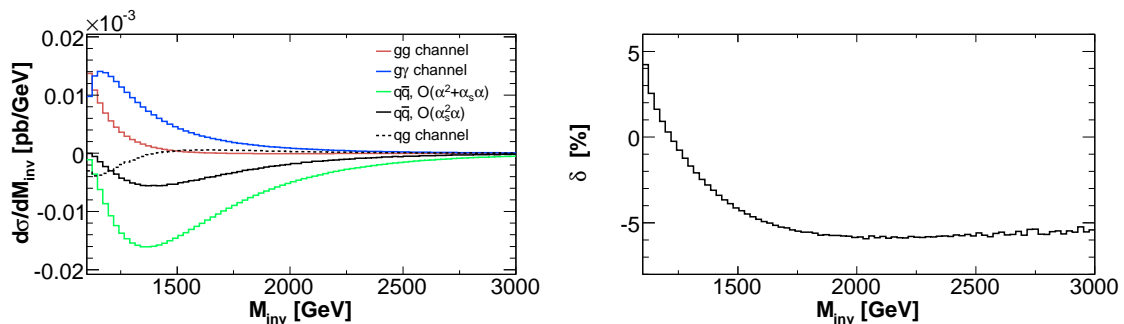


FIGURE 2. Same as Fig. 1 but for $u^R u^{R*}$ production

t -channel gluino exchange.

The on-shell scheme [14, 15] has been used to renormalize masses and wavefunctions of the squarks, of the quarks, and of the gluino. The strong coupling α_s is renormalized in the $\overline{\text{MS}}$ scheme. The contribution of the massive particles (top, squarks, and gluino) to the running of α_s has been subtracted at zero momentum transfer. Dimensional regularization spoils SUSY at higher order; at one loop SUSY can be restored by adding a finite counterterm for the renormalization of the squark-quark-gluino Yukawa coupling.

Real Corrections

IR and collinear finite results are obtained including the processes of real photon emission. In the case of $q\bar{q}$ annihilation real gluon emission of $\mathcal{O}(\alpha_s^2 \alpha)$ has to be considered as well. The treatment of IR and collinear divergences has been performed using two different methods: phase space slicing and dipole subtraction [16]. They give results in good numerical agreement.

IR singularities drop out in the sum of virtual and real corrections. Surviving collinear singularities have to be factorized and absorbed into the definition of the PDF of

the quarks.

Other contributions of $\mathcal{O}(\alpha_s^2 \alpha)$ arise from the processes of real quark emission from quark-gluon fusion. These contributions exhibit divergences when the outgoing quark is emitted collinearly to the gluon. Such singularities are extracted using the two aforementioned methods and have been absorbed into the PDFs. In specific SUSY scenarios, the internal-state gauginos can be on-shell. The poles in the resonant propagators are regularized introducing the width of the corresponding particle.

NUMERICAL RESULTS

For illustration of the EW effects, we study the pair production of the squarks $\tilde{u}^R, \tilde{u}^L, \tilde{d}^L$ and \tilde{c}^L , focusing on the SPS1a' point of the MSSM parameter space, suggested by the SPA convention [17]. A more comprehensive analysis can be found in ref. [9].

Figs. 1–4 contain the invariant mass distribution of the squark-anti-squark pair for the different squark species. In the low invariant mass region EW corrections are positive, decreasing as M_{inv} increases and becoming negative in the high invariant mass region. The contribution of the $\gamma\gamma$ channel is independent on the chirality of the

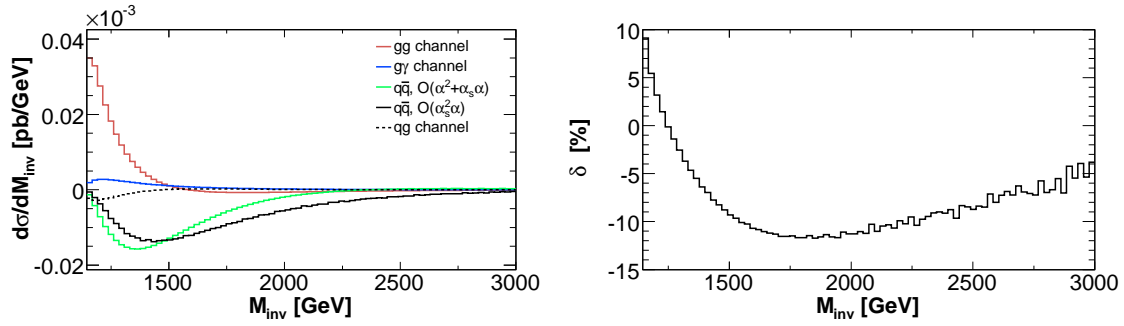


FIGURE 3. Same as Fig. 1 but for $d^L d^{L*}$ production

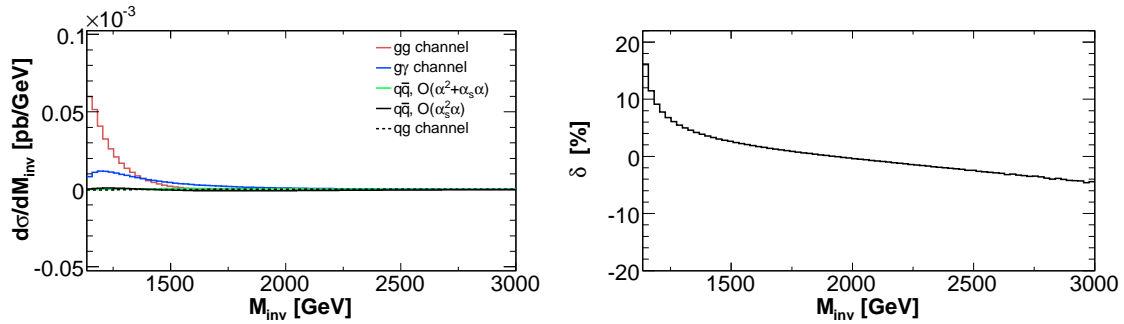


FIGURE 4. Same as Fig. 1 but for $c^L c^{L*}$ production

produced squark, determined only by its charge. In the case of production of same-chirality and same-isospin squarks, e.g. $u^L u^{L*}$ and $c^L c^{L*}$, the corresponding contributions of gg and $\gamma\gamma$ channels are equal (c.f. Fig. 1 and Fig. 4), owing to the mass degeneracy of the produced squarks¹. Comparing Fig. 1 and Fig. 4, one can understand the key role of the $q\bar{q}$ annihilation channels when the quark belongs to the same $SU(2)$ doublet of the produced squark. In the case of $u^L u^{L*}$ production the contribution of these channels is negative and sizeable while in the case of $c^L c^{L*}$ production it is suppressed by the PDFs rendering the impact of the $q\bar{q}$ channels negligible.

REFERENCES

1. P. R. Harrison, and C. H. Llewellyn Smith, *Nucl. Phys.* **B213**, 223 (1983).
2. H. Baer, and X. Tata, *Phys. Lett.* **B160**, 159 (1985).
3. E. Reya, and D. P. Roy, *Phys. Rev.* **D32**, 645 (1985).
4. S. Dawson, E. Eichten, and C. Quigg, *Phys. Rev.* **D31**, 1581 (1985).
5. W. Beenakker, R. Hopker, M. Spira, and P. M. Zerwas, *Nucl. Phys.* **B492**, 51–103 (1997), hep-ph/9610490.

6. S. Bornhauser, M. Drees, H. K. Dreiner, and J. S. Kim, *Phys. Rev.* **D76**, 095020 (2007), 0709.2544.
7. W. Hollik, M. Kollar, and M. K. Trenkel, *JHEP* **02**, 018 (2008), 0712.0287.
8. M. Beccaria, G. Macorini, L. Panizzi, F. M. Renard, and C. Verzegnassi (2008), 0804.1252.
9. W. Hollik, and E. Mirabella (2008), 0806.1433.
10. T. Hahn, *Comput. Phys. Commun.* **140**, 418–431 (2001), hep-ph/0012260.
11. T. Hahn, and C. Schappacher, *Comput. Phys. Commun.* **143**, 54–68 (2002), hep-ph/0105349.
12. T. Hahn, and M. Perez-Victoria, *Comput. Phys. Commun.* **118**, 153–165 (1999), hep-ph/9807565.
13. T. Hahn, and M. Rauch, *Nucl. Phys. Proc. Suppl.* **157**, 236–240 (2006), hep-ph/0601248.
14. W. Hollik, and H. Rzehak, *Eur. Phys. J.* **C32**, 127–133 (2003), hep-ph/0305328.
15. A. Denner, *Fortschr. Phys.* **41**, 307–420 (1993), 0709.1075.
16. S. Dittmaier, *Nucl. Phys.* **B565**, 69–122 (2000), hep-ph/9904440.
17. J. A. Aguilar-Saavedra, et al., *Eur. Phys. J.* **C46**, 43–60 (2006), hep-ph/0511344.

¹ Such degeneracy arises because quarks belonging to the first two generations are treated as massless.